AGU PUBLICATIONS

Water Resources Research

RESEARCH ARTICLE
10.1002/2014WR015362

Special Section:
Eco-hydrology of Semiarid Environments: Confronting Mathematical Models with Ecosystem Complexity

Effects of heterogeneous soil-water diffusivity on vegetation pattern formation

H. Yizhaq[1,2], S. Sela[3], T. Svoray[3], S. Assouline[4], and G. Bel[1]

[1]Department of Solar Energy and Environmental Physics, Blaustein Institutes for Desert Research, Ben-Gurion University of the Negev, Sede Boqer Campus, Israel, [2]The Dead Sea and Arava Science Center, Tamar Regional Council, Israel, [3]Department of Geography and Environmental Development, Ben-Gurion University of the Negev, Beer-Sheva, Israel, [4]Department of Environmental Physics and Irrigation, Agricultural Research Organization, Bet Dagan, Israel

Key Points:
- Modeling the effects of heterogeneous soil-water diffusivity
- Heterogeneity increases vegetation durability
- Vegetation pattern changes from self-organized to imposed due to heterogeneity

Correspondence to:
G. Bel,
bel@bgu.ac.il

Citation:
Yizhaq, H., S. Sela, T. Svoray, S. Assouline, and G. Bel (2014), Effects of heterogeneous soil-water diffusivity on vegetation pattern formation, *Water Resour. Res.*, *50*, doi:10.1002/2014WR015362.

Received 27 JAN 2014
Accepted 25 JUN 2014
Accepted article online 27 JUN 2014

Abstract Many mathematical models have been proposed to explain the emergence of vegetation patterns in arid and semiarid environments, but only a few of them take into account the heterogeneity in the system properties. Here we present a rigorous study of the effects of heterogeneous soil-water diffusivity on vegetation patterns, using two mathematical models. The two models differ in the pattern-forming feedback that they capture; one model captures the infiltration contrast between vegetated and bare-soil domains, whereas the other model captures the increased growth rate of denser vegetation due to an enhanced ability to extract water from the soil. In both models, the most significant effect of the heterogeneity on the soil-water diffusivity is the increased durability of patterned vegetation to a reduced precipitation rate. An additional effect is that the heterogeneity makes the desertification process, namely, the transition from a spotted vegetation pattern to a bare-soil state, more gradual than in the homogeneous system. Our findings suggest that the heterogeneity cannot be neglected in the study of critical transitions in heterogeneous ecosystems and, particularly, in the study of the desertification process due to climate changes or anthropogenic disturbances.

1. Introduction

Vegetation patterns have been observed in many dry environments around the world, including Africa, Australia, North and South America, and Asia (see Figure 1) [*Deblauwe et al.*, 2008; *Borgogno et al.*, 2009]. Many mathematical models have been developed to explain these fascinating phenomena. The common view is that the vegetation patterns reflect a spatial self-organization resulting from a symmetry-breaking instability, which drives the uniform system out of equilibrium [*Meron*, 2012]. The symmetry-breaking instability occurs only when the feedbacks, destabilizing the uniform state, overcome the stabilizing mechanisms. The basic ingredients of many of the mathematical models describing the vegetation dynamics are the local or short-range facilitation and the long-range competition for the limiting resource–water. The facilitation mechanisms include the infiltration contrast, the water-uptake rate and the root augmentation [*Meron*, 2012]. The infiltration feedback represents the increased infiltration rate of surface water in vegetated patches due to the modification of the local soil properties by plants [*D'Odorico et al.*, 2007; *Bedford and Small*, 2008]. The resulting higher soil-water content increases the vegetation growth rate. The root-augmentation feedback represents the coupling between the growth of the root system's girth and the growth of the aboveground vegetation. The extended root zone allows the vegetation to extract soil water from a larger area [*Schenk and Jackson*, 2002; *Casper et al.*, 2003], which, in turn, enhances the growth rate. The water-uptake feedback represents the fact that denser vegetation can extract soil water more efficiently, thereby increasing the vegetation growth rate. The increased amount of water used by the vegetation is extracted from neighboring domains, thereby inhibiting the vegetation growth in bare-soil areas. The combination of local or short-range positive feedbacks and long-range competition for water leads to a finite wave number instability of the uniform vegetation cover state and to the emergence of patterns. The patchiness of the system allows resource concentration, and the produced biomass, per unit area, increases compared to a uniform vegetation cover [*Noy-Meir*, 1973]. Although different models consider different physical mechanisms, they all predict the same five basic vegetation states along a decreasing rainfall gradient—uniform vegetation cover, vegetation cover interspersed with gaps of bare soil, vegetation stripes, vegetation spots, and uniform bare soil [*Borgogno et al.*, 2009; *Meron*, 2012]—and the existence of a bistability range for each pair of consecutive states, e.g., bistability of stripes and spots [*Gilad et al.*, 2004].

Recent studies have shown that climate variability, in particular, the intermittency of precipitation in arid regions, may also lead to the formation of patterned vegetation [*Rodríguez-Iturbe and Porporato*, 2004; *D'Odorico et al*., 2007; *Katul et al*., 2007; *Good and Caylor*, 2011; *Franz et al*., 2012]. The stochasticity of the precipitation can result in vegetation patterns even under conditions in which the feedbacks between vegetation and water are not strong enough to destabilize the uniform vegetation state [*D'Odorico et al*., 2007].

In all the deterministic models mentioned above, a critical transition from the spot-patterned state to the bare-soil state is observed when the precipitation rate decreases [*Zelnik et al*., 2013]. While all the models predict the same vegetation patterns, they differ in the predicted range of the patterns existence and multistability and in the spatial dimension of the pattern. In addition, the relationship between the soil water and the vegetation biomass pattern depends on the feedbacks considered in the specific model [*Zelnik et al*., 2013].

The critical transitions predicted by the vegetation models and other nonlinear models have been the focus of many studies. Different scenarios of regime shift, due to climate changes or anthropogenic disturbances [*Rietkerk et al*., 2004; *Borgogno et al*., 2009], have been investigated. Various examples of the abrupt response of ecosystems have been reported, including the sudden increase in water turbidity and the decrease in vegetation cover in shallow lakes subject to human-induced eutrophication, coral reefs overgrown by fleshy macroalgae, and desertification induced by climate changes or human disturbances [*Reynolds et al*., 2007]. Changes in the states of ecosystems strongly affect human life. Therefore, vigorous research efforts, aimed at devising early indicators of impending degradation processes [*Dakos et al*., 2011; *Kéfi et al*., 2011], have been undertaken.

Most of the models assume that the system is spatially homogeneous, which means that the parameters are spatially uniform and that the vegetation patchiness is a result of the positive feedback between plant biomass and water. However, soil properties and observed vegetation patterns in dry environments are extremely heterogeneous [*Svoray and Karnieli*, 2011]. The heterogeneity arises from small changes in the soil texture and composition, the presence of small rocks and stones that modify the infiltration and flow of surface water [*Creda*, 2001; *Katra et al*., 2008], microtopography [*Noy-Meir*, 1973; *Pelletier et al*., 2012; *Schlesinger et al*., 1996], changes in soil depth [*Sela et al*., 2012] (see Figure 2), changes in the slope [*Svoray et al*., 2008], the spatial distribution of nutrients [*Cambardella et al*., 1994], and many other factors [*Mulla and McBratney*, 1999] that increase the complexity of the system. Despite the extensive studies of vegetation patterns by mathematical models, only a few of them were devoted to the study of the influence of spatial heterogeneity on the pattern formation. In a recent work [*Sheffer et al*., 2013], the heterogeneity was modeled by assuming a patch of soil surrounded by rocks. Namely,

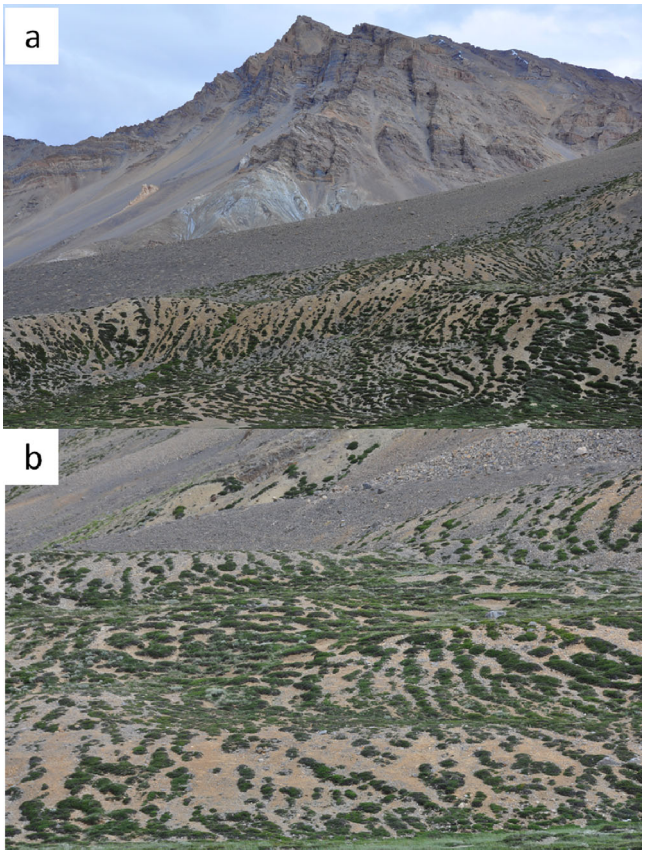

Figure 1. Examples of vegetation patterns in Ladakh, India (32° 53′ 24″ N, 77° 31′ 48″ E) at an altitude of 4500 m above sea level. The mean annual precipitation in this area is less than 200 mm/yr. The vegetation patterns show a mix of bands and spots.

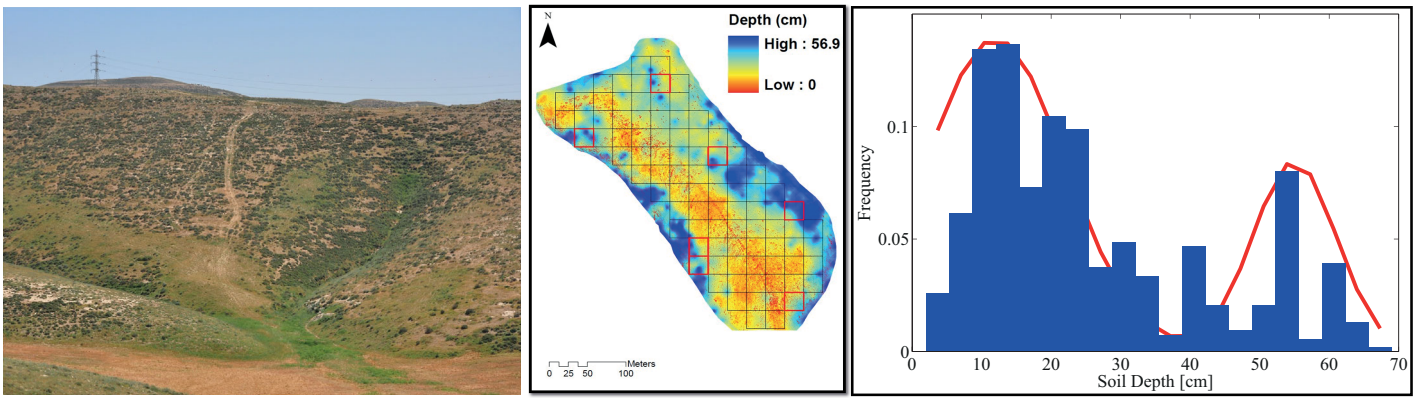

Figure 2. Soil depth heterogeneity in the Lehavim LTER in the northern Negev (mean annual precipitation is 290 mm). (left) The site from which the data was collected. (middle) A map of extrapolated soil depth measurements from a hillslope representing the LTER conditions. (right) A histogram of the soil depth based on 535 measurements (the red line shows a fit to a linear combination of two Gaussian probability density functions). The data demonstrate the significance of heterogeneity in soil characteristics in modeling vegetation dynamics.

the simulated domain consisted of an area, in which the infiltration rate was nonzero, and a surrounding area, in which the infiltration rate was zero. In other words, they considered two neighboring domains with different infiltration rate values. Their results showed that the vegetation pattern was affected by the interplay between the characteristic length of the self-organized vegetation pattern and the length of the domain with a nonzero infiltration rate. The critical transitions in this system were not studied. In *van Nes and Scheffer* [2005], the effects of heterogeneity on the critical transition in a system exhibiting two uniform stable states were studied. It was shown that heterogeneity with short-range spatial correlations does not affect the system dynamics considerably. Heterogeneity with long-range spatial correlations was shown to make the transition between the alternative stable states more gradual. For the effect to be significant, the coupling between neighboring domains has to be strong. To the best of our knowledge, the effects of soil and water heterogeneity on the dynamics of pattern-forming vegetation and, in particular, on the regime shifts in these systems have not been studied. Here we study quantitatively how the spatial variability in one of the model's parameters (soil-water diffusivity) affects the vegetation patterns and the critical transition to the bare-soil state.

2. Methods

In what follows, we use two models describing the dynamics of water-limited vegetation. The two models differ in the pattern-forming feedback that they capture. The first model is the well-studied model introduced by *Rietkerk et al.* [2002, 2004] [*Kéfi et al.*, 2010]. We will refer to this model as the R model in what follows. This model captures the infiltration feedback, namely the higher infiltration rate of surface water in vegetated patches. The higher soil-water density increases the growth rate of the vegetation and drives the instability of the uniform state to nonuniform perturbations (finite wave number instability). This feedback results in patterns of vegetation and soil-water densities that are "in-phase." Specifically, the soil-water density is maximal in spots in which the vegetation density is maximal. The infiltration feedback is expected to be dominant in clayey soil landscapes where physical or biological soil crust tends to form and reduce the surface-water infiltration [*Assouline*, 2004; *Belnap*, 2006]. The vegetation increases the porosity of the soil and prevents the growth of the crust, thereby, increasing the surface-water infiltration rate [*Rietkerk et al.*, 1997; *Rietkerk*, 1998; *Rietkerk et al.*, 2002; *Segoli et al.*, 2008]. The second model (the VSG model) is a simplified version of the model introduced by *Gilad et al.* [2004, 2007]. The model of *Gilad et al.* [2004, 2007] captures two pattern-forming feedbacks: the infiltration feedback (explained above) and the root-augmentation feedback. The root-augmentation feedback reflects the fact that the root system of vegetation laterally expands as the vegetation grows, thereby allowing it to extract water from a larger area. The VSG model simplifies the model of *Gilad et al.* [2004, 2007] using two assumptions. First, it assumes that the infiltration feedback is negligible. This assumption is well-justified in sandy soils located in areas where the climate conditions prevent the formation of crust [for example, *Juergens*, 2013 work shows no evidence for an infiltration contrast between vegetated patches and bare-soil domains]. The second assumption is that

the lateral extent of the root zone is smaller than the typical size of the aboveground vegetation patch. This assumption allows us to replace the nonlocal, root-augmentation feedback with the local water-uptake feedback [*Zelnik et al*., 2013; *Kinast et al*., 2014]. Namely, we assume that the root system develops mostly vertically, thereby increasing the ability of the vegetation to extract water from the soil without expanding to larger areas. The assumption regarding the root system is valid for various perennial grasses, e.g., *Stipagrostis Ciliata*, which forms patterns with a typical length scale of 10 m [*Picker et al*., 2012] and has a root girth of approximately 0.5 m [*Midgley and van der Heyden*, 1999]. When the soil-water diffusivity is large enough, the water-uptake feedback results in an instability of the uniform vegetation state to nonuniform perturbations (finite wave number instability). The VSG model causes vegetation and soil-water patterns to have an "anti-phase" relation. Namely, the soil-water content is minimal in patches where the vegetation density is maximal (see, for example, *Juergens* [2013]; in the sandy environment studied, it is shown that the soil-water content is higher in bare spots).

The soil-water diffusivity has an opposite effect on the two mechanisms. In the R model, it weakens the pattern-forming feedback by allowing the soil water to diffuse away from the vegetation patches. On the other hand, in the VSG model, a large soil-water diffusivity is essential for the water-uptake feedback. A large soil-water diffusivity is required in order to allow a rapid enough soil-water flow toward the vegetation patches. The use of both models will allow us to compare the effects of the heterogeneous soil-water diffusivity on both mechanisms of pattern formation. It is important to note that both models describe the dynamics of long-time scales and the effects of seasonal changes in the precipitation rate, and other climatic conditions are not well captured in the model. As we mentioned in the introduction, other models showed that when the relevant time scales are resolved by the model, the intermittency of the precipitation is an important mechanism in vegetation pattern formation [*Rodríguez-Iturbe and Porporato*, 2004; *D'Odorico et al*., 2006, 2007; *Katul et al*., 2007; *Good and Caylor*, 2011; *Franz et al*., 2012]. The effects of temporal stochasticity in the precipitation rate, although important [*Schwinning and Sala*, 2004], are beyond the scope of the current paper. Other effects that are neglected in our models are the feedbacks of the vegetation on the erosion of the soil and the sediment and nutrient distributions [*Puigdefabregas et al*., 1999; *Puigdefabregas*, 2005; *Saco and Moreno-de las Heras*, 2013]. More detailed descriptions of the models follow.

2.1. The R Model

The R model describes the spatiotemporal dynamics of the surface-water H, soil-water W, and vegetation areal densities B. The areal density of the surface water is fully determined by the height of the water layer above the surface. The soil-water areal density represents the mass of water and moisture in the layers accessible to the vegetation root systems per unit area. It is related to the fractional water content and to the depth of the wet/moist soil layers. The vegetation areal density depends on the height of the vegetation and also on the volumetric density of the vegetation. All three densities are measured in units of mass per area—kilograms per square meter (kg/m^2). The coupled dynamics of these variables is described by the following set of equations:

$$\frac{\partial B}{\partial t} = cg_{\max}\frac{W}{W+k_1}B - dB + D_b\nabla^2 B, \tag{1}$$

$$\frac{\partial W}{\partial t} = \alpha\frac{B+k_2 w_0}{B+k_2}H - g_{\max}\frac{W}{W+k_1}B - r_w W + D_w\nabla^2 W, \tag{2}$$

$$\frac{\partial H}{\partial t} = R - \alpha\frac{B+k_2 w_0}{B+k_2}H - I_0 H + D_h\nabla^2 H. \tag{3}$$

The spatiotemporal dynamics of the vegetation is affected by the growth, mortality, and spatial expansion of the vegetation. The growth term, $cg_{\max}\frac{W}{W+k_1}B$, assumes that the growth is a rate process (and thus proportional to B) and that the growth rate is proportional to the soil-water-uptake rate, which in turn depends on the soil-water density. c is a dimensionless parameter describing the ratio between the vegetation growth rate and the water-uptake rate $g_{\max}\frac{W}{W+k_1}$. $g_{\max}$ is the maximal water-uptake rate, and its units are 1/day. For low soil-water density ($W \ll k_1$), the water-uptake rate is proportional to the soil-water density, while for high density ($W \gg k_1$), the water-uptake rate saturates (the maximal vegetation growth rate is cg_{max}, and it corresponds to conditions in which the growth limiting factor is not the availability of water). The vegetation also experiences natural mortality with a rate d (d is also measured in units of 1/day). The

mortality term, $-dB$, reflects the assumption that the mortality rate is independent of the vegetation, surface-water, and soil-water densities. The spatial expansion of the vegetation, due to clonal growth or seed dispersion, is described by the diffusion term, $D_b\nabla^2 B$, and its magnitude is characterized by the vegetation diffusion coefficient, D_b (measured in units of m^2/day). The dynamics of the soil-water density is affected by several processes: (i) the vegetation water-uptake rate (the term $g_{max}WB/(W+k_1)$); (ii) the evaporation and drainage of soil water (the term $-r_wW$, which is characterized by the rate r_w; r_w is measured in units of 1/day); (iii) the infiltration of surface water. The term $\alpha\frac{B+k_2w_0}{B+k_2}H$ represents the fact that the total infiltration is proportional to the surface-water density, H, and the dependence of the infiltration rate on the vegetation density as it grows from αw_0 in bare soil ($B=0$) to α for very dense vegetation ($B \gg k_2$); α is the maximal infiltration rate (it is measured in units of 1/day); w_0 is a dimensionless parameter characterizing the ratio between the surface-water infiltration rate in bare soil and the infiltration rate in densely vegetated domains; k_2 represents the vegetation areal density at which the infiltration rate saturates (for $B=k_2$, the infiltration rate is equal to $\alpha(1+w_0)/2$, which is the average of the maximal and minimal infiltration rates) (k_2 has the same dimension as the vegetation areal density (kg/m^2)); and (iv) the diffusion of soil water, which is characterized by the soil-water diffusivity, D_w (measured in units of m^2/day). The surface-water dynamics is affected by (i) the precipitation (with rate R measured in $kg/m^2/day$, which is equivalent to mm/day if we set the water density to $1000kg/m^3$); (ii) the infiltration of surface water (the term $\alpha\frac{B+k_2w_0}{B+k_2}H$; see the explanation above for details); (iii) the evaporation rate and losses due to the runoff of surface water (the term $-l_0H$), which are characterized by a single rate l_0 (this term was introduced to allow for the bistability of two uniform states [*Kéfi et al*., 2010]); and (iv) the diffusion of surface water (with diffusivity D_h, measured in units of m^2/day). We assume plain topography, and therefore, the surface water transport is assumed to be dominated by the diffusion rather than by the flow in the direction of the slope. The infiltration feedback (namely, the increased infiltration of surface water in denser vegetation patches) represents the fact that vegetation cracks the soil crust that is found in many arid regions. The soil crust reduces the infiltration of surface water, and therefore, the cracking by the vegetation and its root system results in a higher surface-water infiltration rate [*Walker et al*., 1981; *van Wijngaarden*, 1985; *Rietkerk et al*., 1997; *Rietkerk*, 1998; *Rietkerk et al*., 2002; *Segoli et al*., 2008]. Therefore, the R model is suitable for describing vegetation dynamics in clayey soil landscapes. In what follows, we use the scaled soil-water diffusivity, $\delta_w \equiv D_w/D_b$, scaled biomass density, $b \equiv B/k_2$, and scaled soil-water density, $w \equiv W/k_1$, all of which are dimensionless.

The effects of heterogeneity in this model were investigated by introducing spatially nonuniform, soil-water diffusivity. The diffusivity at each point was drawn from a Gaussian distribution

$$p(\delta_w)=\frac{1}{\sqrt{2\pi\sigma^2}}\exp\left(-\frac{(\delta_w-<\delta_w>)^2}{2\sigma^2}\right), \tag{4}$$

where $\langle\delta_w\rangle$ is the mean value and σ is the standard deviation of the scaled soil-water diffusivity. In general, the Gaussian probability density function allows negative values, which are not physical. Therefore, negative values were replaced by the mean value. The result of this correction is a slightly narrower distribution and a mean value that is slightly larger than $\langle\delta_w\rangle$. In all of the realizations that we used in this work, we verified that these deviations from the mean and the standard deviation were negligible. It is important to note that we neglected the spatial correlations of the soil-water diffusivity, and we assumed that the diffusivity in each grid cell is independent of the diffusivity in the neighboring cells. In Figure 3, we show representative realizations of the heterogeneity for different values of the standard deviation. The model equations were numerically integrated using an explicit fourth-order, finite difference scheme with no-flux boundary conditions and with a second order Adam-Bashforth scheme for the time integration. The grid consisted of 128×128 cells, the spatial resolution was 2 m, and the temporal resolution was 0.001 days. The model parameters we used are similar to the parameters used in *Kéfi et al*. [2010] and are provided in Table 1.

These parameters correspond to clayey soil (strong infiltration contrast) [*Anderson and Hodgkinson*, 1997; *Bromley et al*., 1997]. The precipitation rate and the standard deviation of the soil-water diffusivity varied, and they are specified for each result.

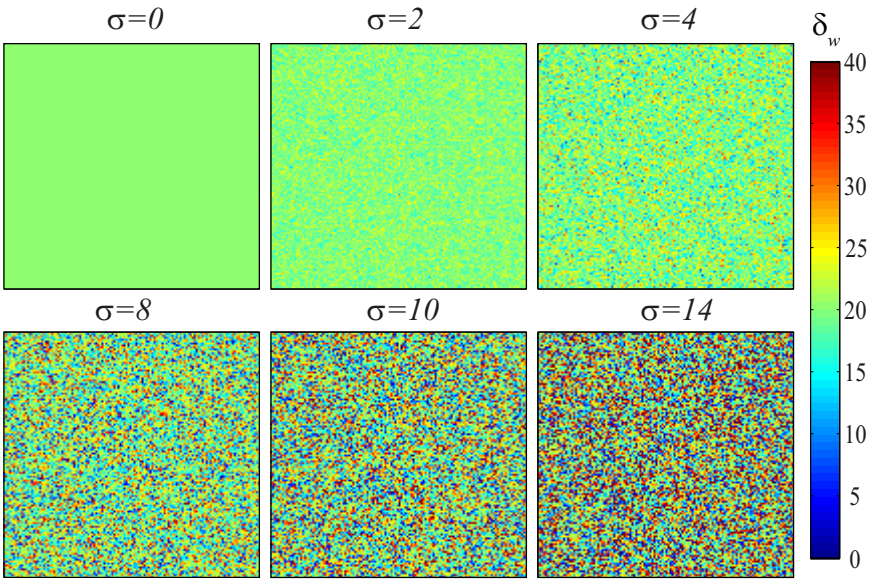

Figure 3. Representative realizations of the heterogeneity in δ_w that we used in the R model simulations. The different plots correspond to different values of the standard deviation, σ, of the Gaussian probability density function with $<\delta_w> = 20$.

2.2. The VSG Model

The VSG model describes the spatiotemporal dynamics of only two variables, the vegetation areal density, B, and the soil-water areal density, W. The model equations are

$$\frac{\partial B}{\partial t} = \Lambda WB(1-B/k)(1+EB)^2 - Mb + D_b\nabla^2 B, \tag{5}$$

$$\frac{\partial W}{\partial t} = p - N(1-\rho B/k)W - \Gamma(1+EB)^2 WB + D_w\nabla^2 W. \tag{6}$$

This model uses a logistic growth term for the vegetation, $\Lambda WB(1-B/k)(1+EB)^2$. The growth term is proportional to the soil-water extraction flux, $\Gamma(1+EB)^2W$ (measured in units of $kg/m^2/yr$), and it reflects the nonlinear growth of the soil-water extraction with the vegetation density (see *Kinast et al.* [2014] for more details). The parameter E represents the "root-to-shoot" ratio (we assume here that the root lateral expansion is smaller than the lateral expansion of the aboveground vegetation, and therefore, the term is local and that the soil-water extraction flux grows with the depth and mass of the root system). Λ/Γ is the ratio between the vegetation growth rate and the water extraction rate (the equivalent of the coefficient c in the R model). The vegetation density cannot grow beyond the system's carrying capacity, k, and therefore, the growth term is also proportional to $(1-B/k)$, which decreases the growth rate as the vegetation density

Table 1. Parameters of the R Model

Symbol	Meaning	Value
c	Ratio between the vegetation growth rate and the soil-water-uptake rate	10 (dimensionless)
g_{max}	Maximal water-uptake rate	0.05/day
k_1	Soil-water areal density at which the water-uptake rate is half of the maximal water-uptake rate	5 kg/m^2
d	Vegetation mortality rate	0.25/day
D_b	Vegetation diffusion coefficient	0.1 m^2/day
r_w	Soil-water drainage and evaporation rate	0.2/day
α	Maximal surface-water infiltration rate	0.2/day
k_2	Vegetation areal density at which the surface-water infiltration rate saturates	5 kg/m^2
w_0	The ratio between the infiltration rate in bare soil and the maximal infiltration rate	0.2 (dimensionless)
$\langle D_w \rangle$	Average soil-water diffusivity	0.1 m^2/day
l_0	Evaporation and drainage rate of surface water	0.06/day
D_h	Surface-water diffusion coefficient	100 m^2/day

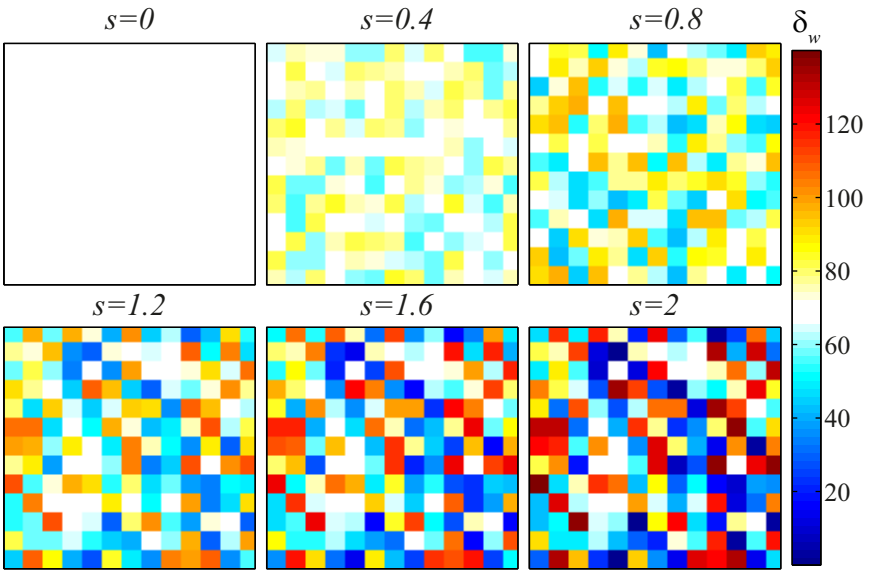

Figure 4. Realizations of the soil-water diffusivity distributions. All plots correspond to uniform distributions of the soil-water diffusivity in the range $\langle\delta_w\rangle(1-s/2) \le \delta_w \le \langle\delta_w\rangle(1+s/2)$ with $\langle\delta_w\rangle=70$.

approaches the system's carrying capacity, k. The vegetation is also affected by the natural mortality, with rate M (measured in units of 1/yr), and by its spatial expansion, due to clonal growth or seed dispersion, characterized by the diffusion coefficient, D_b (measured in units of m^2/yr). The soil-water density dynamics is affected by (i) the precipitation whose rate, p, is measured in units of mass per area per unit time or equivalently in units of mm/yr by assuming that the water density is 1000 kg/m^3; (ii) the water-uptake rate by the vegetation (the term $\Gamma(1+EB)^2WB$, which was explained above); (iii) the diffusion of soil water (the term $D_w\nabla^2W$), which is characterized by the diffusion coefficient, D_w (measured in units of m^2/yr); and (iv) the evaporation and drainage of soil water (the term $-N(1-\rho B/k)W$); N is the evaporation and drainage rate from bare soil. The model also accounts for the shading effect that reduces the evaporation rate in vegetated patches by the amount $\rho B/k$ (ρ is a dimensionless parameter characterizing the reduction in evaporation due to shading by the vegetation). Here again, we introduced the heterogeneity through the spatially nonuniform soil-water diffusivity. For convenience, we used the scaled diffusivity $\delta_w \equiv D_w/D_b$. However, in order to demonstrate the fact that the effects are independent of the distribution of the diffusivity, we used a different distribution from the one used in the R model (equation (4)). δ_w was drawn from the following distribution:

$$p(\delta_w)=\begin{cases} 1/s & \langle\delta_w\rangle(1-s/2) \le \delta_w \le \langle\delta_w\rangle(1+s/2) \\ 0 & else \end{cases}. \tag{7}$$

This is a uniform distribution of δ_w, which we characterized using two parameters. The mean value, $\langle\delta_w\rangle$, which is also the center of the distribution and the range, $\langle\delta_w\rangle(1-s/2) \le \delta_w \le \langle\delta_w\rangle(1+s/2)$. s is related to the standard deviation, σ, by $s=\sqrt{12}\sigma$. The soil-water diffusivity varied between domains of 10×10 grid cells. The response of the system is sensitive to the spatial correlation length. Obviously, for a correlation length longer than the typical length of the pattern formed by the vegetation, the different domains form the corresponding pattern, and there are small changes in the boundaries between the domains. For a correlation length much smaller than the typical length of the self-organized pattern, the heterogeneity is averaged out, and the vegetation pattern is again similar to the pattern formed in a uniform system. For an intermediate correlation length, the interplay between the soil heterogeneity and the self-organized feedbacks affects the system dynamics and stability diagrams. Figure 4 shows the representative realizations of the distribution of δ_w for different values of s. The model equations were numerically integrated using an explicit fourth-order finite difference scheme with periodic boundary conditions and a simple Euler scheme for the time integration. The parameters of the VSG model are provided in Table 2.

Table 2. Parameters of the VSG Model

Symbol	Meaning	Value
Λ	Vegetation growth rate per unit of soil-water density (neglecting the carrying capacity and the water-uptake feedback)	0.004 $m^2/kg/yr$
k	The vegetation carrying capacity (maximal vegetation density in the ecosystem)	0.5 kg/m^2
E	Inverse density of the root system per unit density of the aboveground vegetation	7 m^2/kg
M	Vegetation mortality rate	$0.35/yr$
D_b	Vegetation diffusion coefficient	0.1 m^2/yr
N	Soil-water drainage and evaporation rate from bare soil	$2/yr$
ρ	The fraction of reduced evaporation and drainage due to vegetation	0.5 (dimensionless)
Γ	The rate of soil-water uptake per unit of vegetation areal density	1.5 $m^2/kg/yr$

The precipitation rate, p, the scaled soil-water diffusivity, δ_w, and the width of the probability density function of δ_w, s, varied and are specified for each figure. The grid consisted of 128×128 cells. The spatial resolution was $0.9\sqrt{D_b/M} \approx 0.535$ m. The temporal resolution was $10^{-4}/M \approx 0.104$days. The total area of the grid was 68.5 m$\times$68.5 m. The results of the VSG model are presented using the scaled densities, $b \equiv B/k$ and $w \equiv W\Lambda/N$.

3. Results

Before we turn to study the effects of the heterogeneity, we first examine the effects of changes in the uniform soil-water diffusivity on the patterns formed by the vegetation and the soil-water distribution. In Figure 5, we show the effects of δ_w on the vegetation pattern as predicted by the VSG model. For low values of δ_w (the top left plot in this figure) and a low precipitation rate (p=80 mm/yr), the uniform vegetation cover collapses into the bare-soil state, and no pattern is formed. This is because the water-uptake feedback is not strong enough for low soil-water diffusivity. For higher soil-water diffusivity, a pattern is formed, and the size of the vegetation patches grows with δ_w (for very high values, the patch size saturates). In Figure 6, we show the corresponding soil-water patterns. Note that the vegetation density maxima correspond to the soil-water density minima ("anti-phase" relation). In order to provide a better sense of the global effect of δ_w, we show, in Figure 7, the spatial averages of the vegetation and soil-water densities versus the soil-

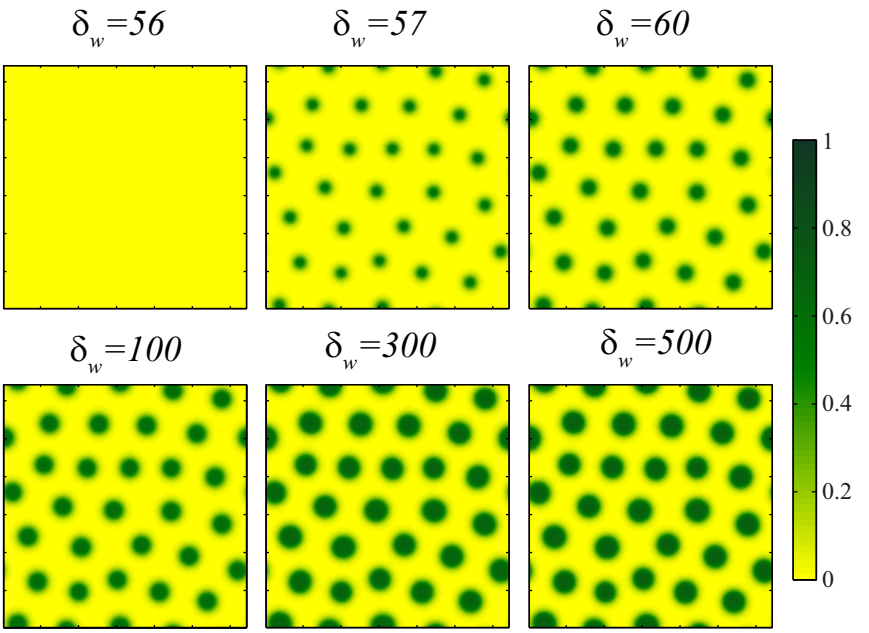

Figure 5. The effect of the soil-water diffusivity on the vegetation pattern in the VSG model. The soil-water diffusivity is uniform. The precipitation rate is p=80 mm/yr. As expected, the larger the soil-water diffusivity, the larger the vegetation spots. When the soil-water diffusivity is too low, the system collapses into the bare-soil state.

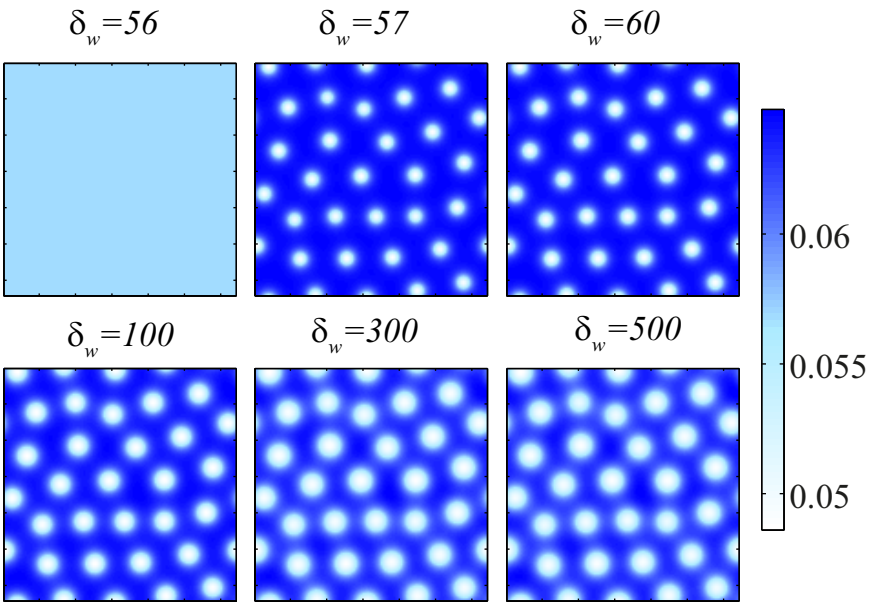

Figure 6. The effect of the soil-water diffusivity on the soil-water pattern in the VSG model. The soil-water diffusivity is uniform. The precipitation rate is $p=80$ mm/yr. As expected, the larger the soil-water diffusivity, the larger the gaps in the soil-water density.

water diffusivity. The leftmost point corresponds to the collapse of the patterns (into the bare-soil state). For very high diffusivity, there is a saturation of both averages. Note that due to the "anti-phase" relationship between the vegetation and the soil-water densities, the average vegetation density decreases as the average soil-water density increases.

In Figure 8, we show the effect of the soil-water diffusivity on the vegetation pattern in the R model. The same growth of the spots with δ_w is observed. However, here the vegetation patches are sparser as the soil-water diffusivity grows. When the diffusivity is too high, the infiltration feedback is no longer effective, and the vegetation pattern disappears. The corresponding soil-water patterns are shown in Figure 9. Note that, here, the vegetation maxima are located at the soil-water maxima ("in-phase" relation). The spatial averages of the soil-water and the vegetation densities are shown in Figure 10. Here similarly to the VSG model, the average soil-water density does not change much with the diffusivity. However, the average vegetation density strongly depends on δ_w. The saturation effect that was seen in the VSG model is not seen here.

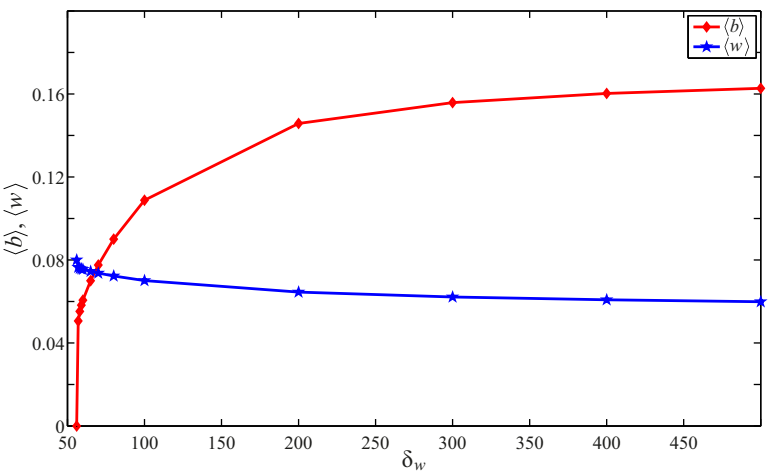

Figure 7. The spatial average of the biomass and soil-water densities ($\langle b\rangle$ and $\langle w\rangle$, respectively) versus the soil-water diffusivity. The soil-water diffusivity is uniform. The precipitation rate is $p=80$ mm/yr.

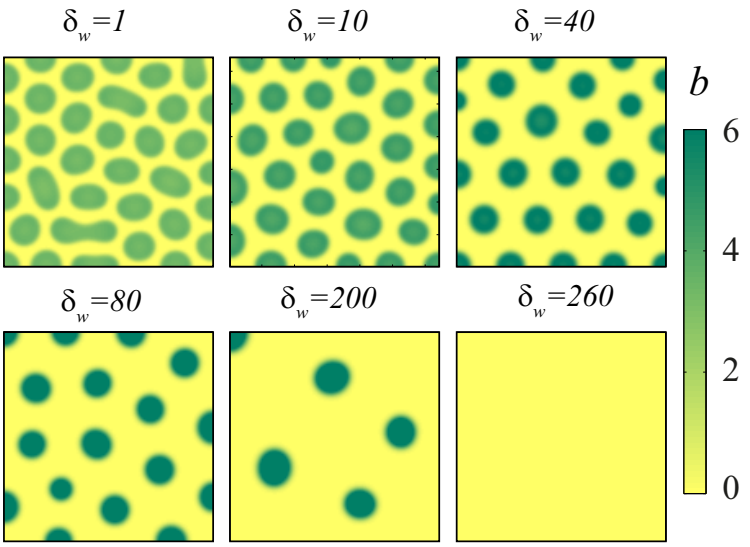

Figure 8. The effect of the soil-water diffusivity on the vegetation pattern in the R model. The soil-water diffusivity is uniform. The precipitation rate is $R=1.56$ mm/day. The larger the soil-water diffusivity, the larger and sparser the vegetation spots. When the soil-water diffusivity is too high, the system collapses into the bare-soil state.

The most obvious effect of the heterogeneity is the change it induced in the patterns formed by the soil-water and the vegetation densities. In both models, an increase in the variance (i.e., stronger heterogeneity) changed the formed pattern toward the pattern imposed by the soil properties rather than the self-organized pattern. Using the VSG model, we show, in Figure 11, the effects of the heterogeneity on the patterns formed by the vegetation. The corresponding soil-water patterns are shown in Figure 12. The effects of the heterogeneity on the vegetation patterns, as predicted by the R model, are shown in Figure 13, and the corresponding soil-water patterns are shown in Figure 14. In the R model, the heterogeneity drives the system from a spotted pattern to a labyrinthine pattern. A very important effect of the heterogeneity is the increased survivability of the vegetation under lower precipitation rates. In Figure 15, we show the bifurcation diagram for different degrees of heterogeneity in the VSG model. The higher the variability of the soil-water diffusivity (quantified by s) the more gradual the transition to the bare-soil state and the lower the

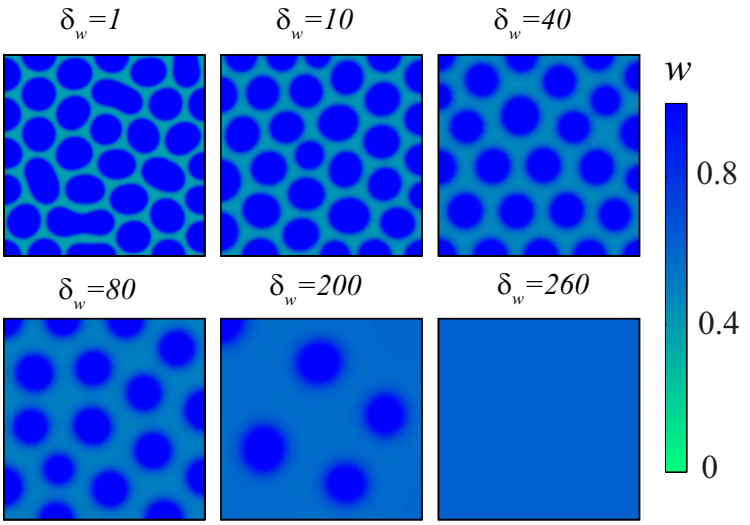

Figure 9. The effect of the soil-water diffusivity on the soil-water pattern in the R model. The parameters are the same as those used in Figure 8. The larger the soil-water diffusivity, the larger the soil-water spots. When the soil-water diffusivity is too high, the vegetation disappears, and the soil-water density becomes uniform.

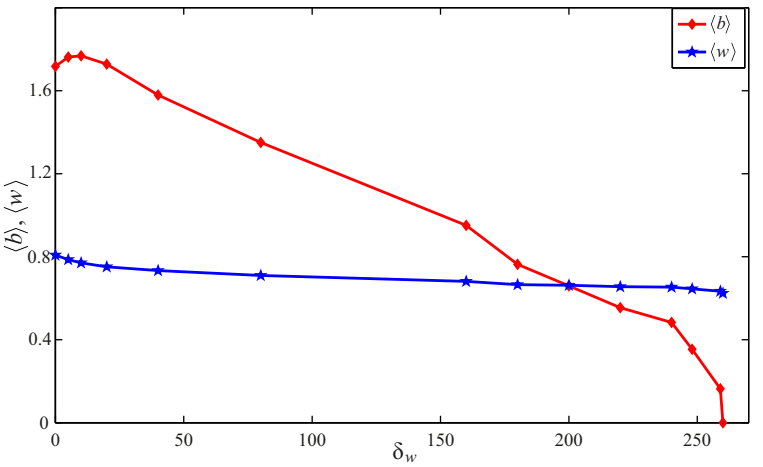

Figure 10. The spatial average of the biomass and soil-water densities versus the soil-water diffusivity in the R model. The soil-water diffusivity is uniform. The precipitation rate is $R=1.56$ mm/day.

precipitation rate at which this transition occurs (the right plot). The left plot shows the corresponding spatial averages of the soil-water density. The nonmonotonic behavior shows that in the absence of vegetation, the soil-water density increases with the precipitation rate, as expected; however, as the vegetation grows and extracts water from the soil, the average soil-water density declines. The inset plots show snapshots of the vegetation pattern at different values of the precipitation rate. Figure 16 shows the same information for the R model.

4. Discussion

Our results show that soil-water diffusivity plays an important role in the dynamics of water-limited vegetation. The transition from a vegetated state to a bare-soil state (often identified with a desertification process [*Reynolds et al*., 2007]) may pass through patterned vegetation states, which persist to lower precipitation rates than the uniform vegetation state. In the mathematical models describing the

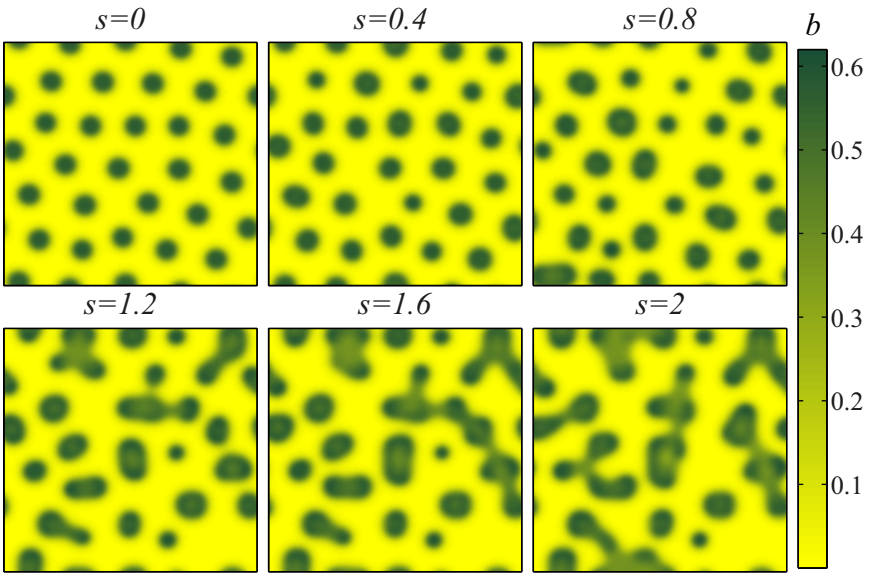

Figure 11. Realizations of the vegetation patterns in the VSG model. All plots correspond to uniform distributions of the soil-water diffusivity in the range $\langle\delta_w\rangle(1-s/2) \le \delta_w \le \langle\delta_w\rangle(1+s/2)$ with $\langle\delta_w\rangle=70$. Large variance of the soil-water diffusivity changes the vegetation pattern significantly.

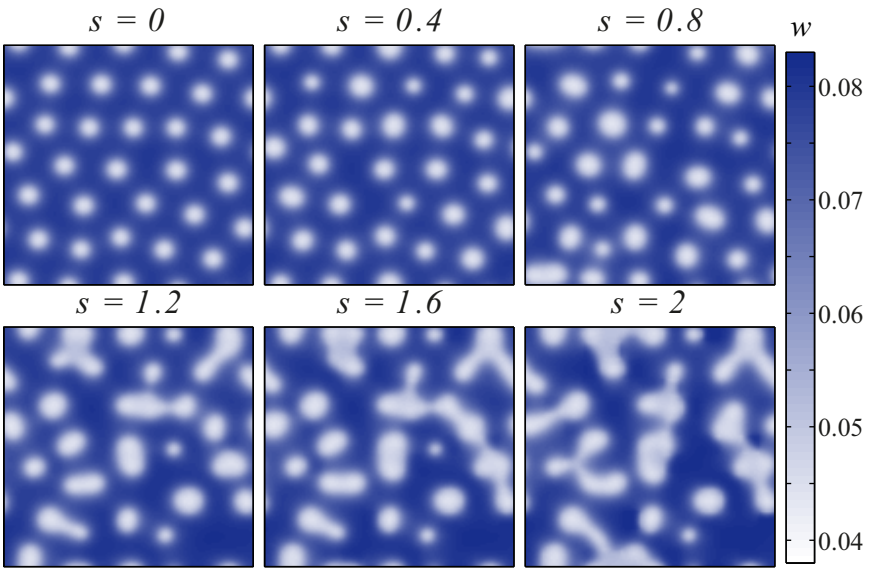

Figure 12. Realizations of the soil-water density in the VSG model. All plots correspond to uniform distributions of the soil-water diffusivity in the range $\langle\delta_w\rangle(1-s/2) \le \delta_w \le \langle\delta_w\rangle(1+s/2)$ with $\langle\delta_w\rangle=70$. Large variance of the soil-water diffusivity changes the soil-water pattern significantly.

vegetation dynamics, the emergence of self-organized vegetation patterns depends on the strength of the feedbacks, which are strongly affected by the soil-water diffusivity. When the dominant feedback is the water uptake, the case modeled using the VSG model, soil-water diffusivity that is too small does not allow the formation of patterns, and the system collapses from the uniform vegetation to the bare-soil state at some critical precipitation rate. In Figures 5 and 6, we show the state of the system under the same climatic conditions but for different values of the soil-water diffusivity. The size of the vegetation spots grows with the diffusivity and eventually saturates. The pattern-forming mechanism in this model is based on the fact that the soil-water density under the vegetation spot is lower than its surroundings. Therefore, the size of the gaps in the corresponding soil-water pattern is similar to the size of

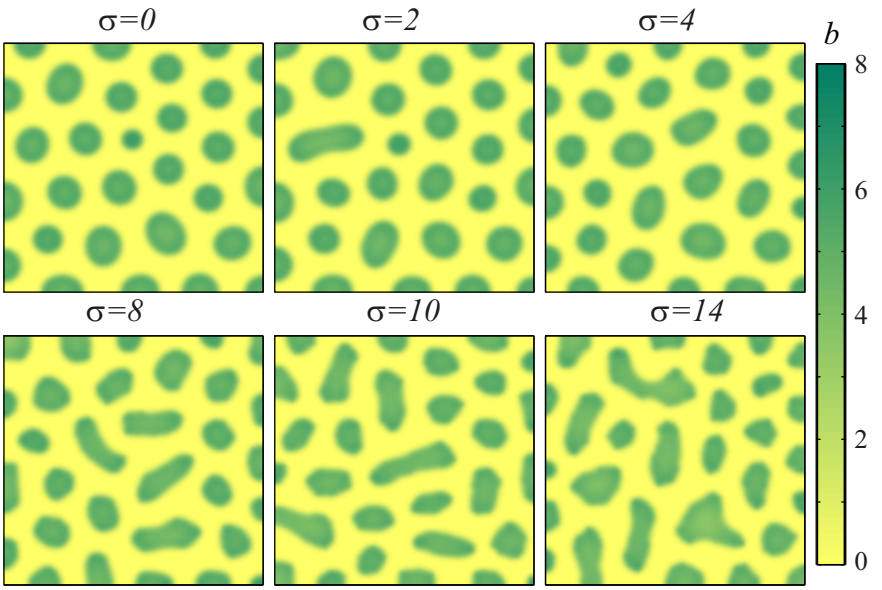

Figure 13. Realizations of the vegetation patterns in the R model. All plots correspond to Gaussian distributions with $\langle\delta_w\rangle=20$ and different values of the standard deviation as specified in this figure. Large variance of the soil-water diffusivity changes the vegetation pattern significantly.

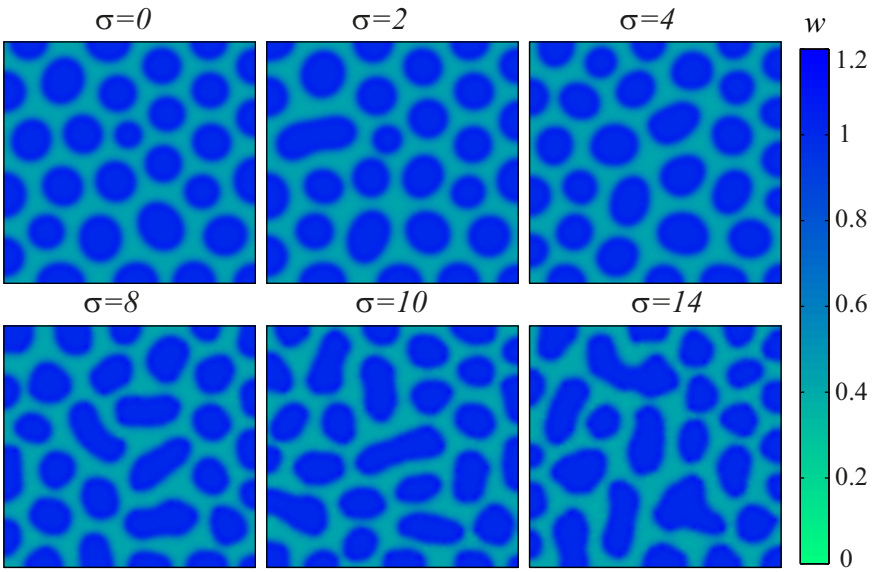

Figure 14. Realizations of the soil-water patterns in the R model. All plots correspond to Gaussian distributions with $\langle\delta_w\rangle=20$ and different values of the standard deviation as specified in this figure. Large variance of the soil-water diffusivity changes the soil-water pattern significantly.

the vegetation spots. Figure 7 shows that for a dominant water-uptake feedback, the average vegetation density grows with the increase of the soil-water diffusivity due to the intensification in the strength of the feedback. Denser vegetation implies a higher water-uptake rate and, therefore, a lower soil-water density as shown in Figure 7. The R model accounts for the infiltration contrast feedback, and it represents the case in which this feedback dominates. In this case, soil-water diffusivity that is too large reduces the strength of the feedback and does not allow the formation of vegetation patterns (see Figure 8). In the R model, the vegetation and soil-water densities are "in phase" (peaks of both quantities occur at the same place), and too large soil-water diffusivity allows the water to diffuse away from the vegetation before it is consumed by it. Thus, in the R model, the size of the soil-water density spots grows significantly with the soil-water diffusivity, as expected (see Figure 9). The averages of both the vegetation and soil-water densities decline with the increase in the soil-water diffusivity, as shown in Figure 10.

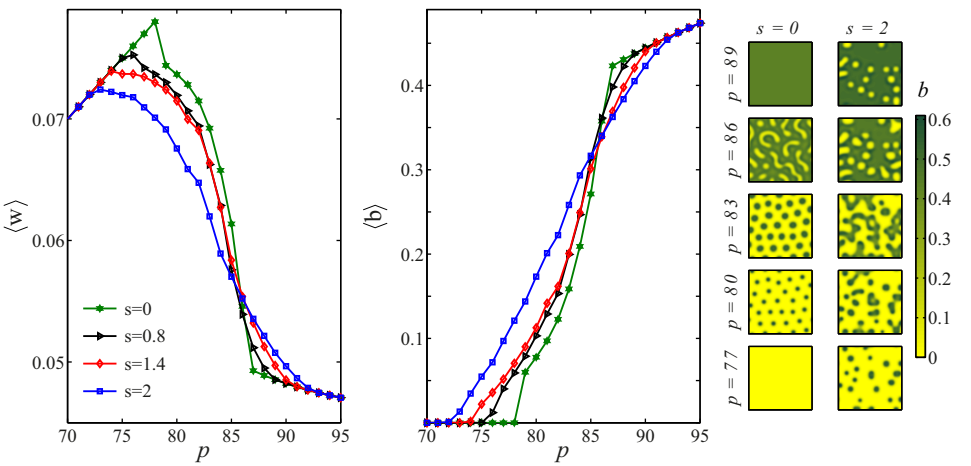

Figure 15. The prediction of the VSG model for the spatial average of the biomass and the soil-water densities ($\langle b\rangle$ and $\langle w\rangle$, respectively) versus the precipitation rate, p (in mm/yr) for different degrees of heterogeneity (measured using the width of the distribution of δ_w, s). All lines correspond to uniform distributions of the soil-water diffusivity in the range $\langle\delta_w\rangle(1-s/2)\le\delta_w\le\langle\delta_w\rangle(1+s/2)$ with $\langle\delta_w\rangle=70$.

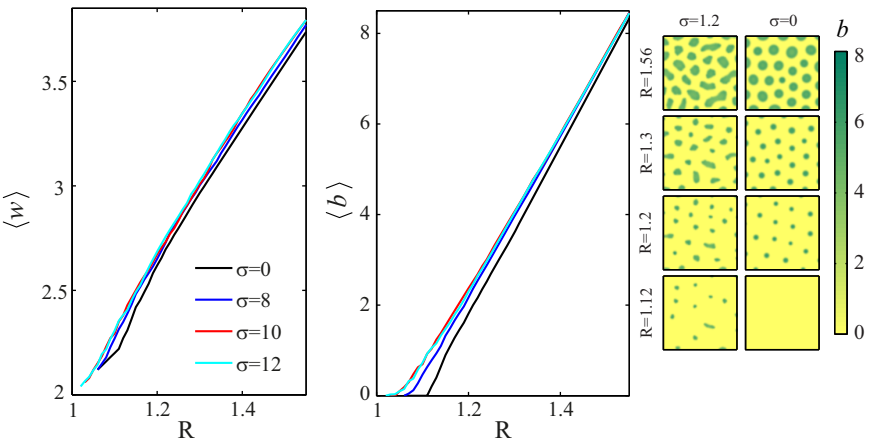

Figure 16. The prediction of the R model for the spatial average of the biomass and the soil-water densities ($\langle b \rangle$ and $\langle w \rangle$, respectively) versus the precipitation rate, R (in mm/day) for different degrees of heterogeneity (measured using the standard deviation of δ_w, σ). All lines correspond to Gaussian distributions of δ_w with $\langle \delta_w \rangle = 20$, and the different values of σ are specified in this figure.

Soil characteristics, including the soil-water diffusivity, are heterogeneous due to spatial changes in the soil composition, porosity, grain-size distribution, and other factors [*Mulla and McBratney*, 1999]. In this work, we assume that the fluctuations in the density of soil-water are sufficiently small, and therefore, we ignore the dependence of the diffusivity on the soil-water density [e.g., *Hillel*, 1998], which means that in the models used here, δ_w does not depend on w. For simplicity, we focus on the heterogeneity of the soil-water diffusivity alone. Figures 11–14 show that the heterogeneity affects the vegetation patterns and the soil-water density. The effects appear in both the R and the VSG models. The plots in Figures 11–14 show that as the heterogeneity increases, the vegetation and soil-water patterns shift from the self-organized pattern into the pattern imposed by the soil heterogeneity. Moreover, for the strong heterogeneity, there is a stable coexistence of different pattern types (such as spots and stripes; see Figure 1), which has never been observed for homogeneous systems.

The most important effect of the heterogeneity is the extended survivability of the ecosystem under climatic changes. Figures 15 and 16 show that for both models, the larger the degree of the heterogeneity, the harsher the climatic conditions that the ecosystem can survive. In addition, the transition between the patterned state and the bare-soil state becomes more gradual. This is easily understood if one takes into account the fact that different domains may respond differently to the external conditions. These additional degrees of freedom soften the transition between the states.

The effect of the heterogeneity on the critical transition is of special interest and relevance to studies aiming to identify early warning signals for imminent regime shifts [*Dakos et al*., 2011; *Kéfi et al*., 2011; *Scheffer et al*., 2009]. The signals based on proximity to the critical point, such as increased variability, skewness, flickering, increased temporal autocorrelation, and critical slowing down near the equilibrium state, are not sufficient for spatially extended ecosystems. Our results show that in spatially extended ecosystems, in which heterogeneity is common, the nature of the transition between alternative stable states may differ significantly from the nature of the transition in a homogeneous system. The heterogeneity may allow the system to respond locally to perturbations, thereby increasing the stability of the system. The diverse responses of different domains make changes in the state of the whole system more gradual. The interplay between different pattern-forming mechanisms [*Kinast et al*., 2014] may also affect the response of the system and the effects of heterogeneity. These effects of the heterogeneity are particularly relevant to desertification in which transitions to the bare-soil state usually take place from spotted vegetation in a heterogeneous ecosystem.

The study presented here is the first step toward a rigorous study of the effects of spatial heterogeneity on the dynamics of pattern-forming systems, in general, and vegetation dynamics, in particular. Future studies may take into account the coupling between the different parameters and the effects of intermittent precipitation.

Acknowledgments
The research leading to these results has received funding from the European Union Seventh Framework Programme (FP7/2007–2013) under grant (293825) and from the Israel Science Foundation (ISF) (grant 1184/11).

References

Anderson, V. J., and K. C. Hodgkinson (1997), Grass-mediated capture of resource flows and the maintenance of banded mulga in a semi-arid woodland, *Aust. J. Bot.*, *45*, 331–342.
Assouline, S. (2004), Rainfall-induced soil surface sealing, *Vadose Zone J.*, *3*, 570–591.
Bedford, D. R., and E. E. Small (2008), Spatial patterns of ecohydrologic properties on a hillslope-alluvial fan transect, central new Mexico rid b-4939-2011, *Catena*, *73*, 34–48.
Belnap, J. (2006), The potential roles of biological soil crusts in dryland hydrologic cycles, *Hydrol. Processes*, *20*, 3159–3178.
Borgogno, F., P. D'Odorico, F. Laio, and L. Ridolfi (2009), Mathematical models of vegetation pattern formation in ecohydrology, *Rev. Geophys.*, *47*, RG1005, doi:10.1029/2007RG000256.
Bromley, J., J. Brouwer, A. P. Barker, S. R. Gaze, and C. Valentin (1997), The role of surface water redistribution in an area of patterned vegetation in a semi-arid environment, southwest Niger, *J. Hydrol.*, *198*, 1–29.
Cambardella, C. A., T. B. Moorman, T. B. Parkin, D. L. Karlen, J. M. Novak, R. F. Turco, and A. E. Konopka (1994), Field-scale variability of soil properties in central Iowa soils, *Soil Sci. Soc. Am. J.*, *58*(5), 1501–1511.
Casper, B. B., H. J. Schenk, and R. B. Jackson (2003), Defining a plant's belowground zone of influence, *Ecology*, *84*, 2313–2321.
Creda, A. (2001), Effects of rock fragment cover on soil infiltration, interrill runoff and erosion, *Eur. J. Soil Sci.*, *52*, 59–68.
Dakos, V., S. Kéfi, M. R. E. H. van Ness, and M. Scheffer (2011), Slowing down in spatially patterned ecosystems at the brink of collapse, *Global Ecol. Biogeogr.*, *77*(6), E153–E166.
Deblauwe, V., N. Barbier, P. Couteron, O. Lejeune, and J. Bogaert (2008), The global biogeography of semi-arid periodic vegetation patterns, *Global Ecol. Biogeogr.*, *17*(6), 715–723.
D'Odorico, P., F. Laio, and L. Ridolfi (2006), Vegetation patterns induced by random climate fluctuations, *Geophys. Res. Lett.*, *33*, L19404, doi:10.1029/2006GL027499.
D'Odorico, P., K. Caylor, G. S. Okin, and T. M. Scanlon (2007), On soil moisture-vegetation feedbacks and their possible effects on the dynamics of dryland ecosystems, *J. Geophys. Res.*, *112*, G04010, doi:10.1029/2006JG000379.
Franz, T. E., K. K. Caylor, E. G. King, J. M. Nordbotten, M. A. Celia, and I. Rodriguez-Iturbe (2012), An ecohydrological approach to predicting hillslope-scale vegetation patterns in dryland ecosystems, *Water Resour. Res.*, *48*, W01515, doi:10.1029/2011WR010524.
Gilad, E., J. von Hardenberg, A. Provenzale, M. Shachak, and E. Meron (2004), Ecosystem engineers: From pattern formation to habitat creation, *Phys. Rev. Lett.*, *93*, 098105.
Gilad, E., J. von Hardenberg, A. Provenzale, M. Shachak, and E. Meron (2007), A mathematical model for plants as ecosystem engineers, *J. Theor. Biol.*, *244*, 680–691.
Good, S. P., and K. K. Caylor (2011), Climatological determinants of woody cover in Africa, *Proc. Natl. Acad. Sci. U. S. A.*, *108*, 4902–4907.
Hillel, D. (1998), *Environmental Soil Physics*, Academic Press, San Diego, Calif.
Juergens, N. (2013), The biological underpinnings of Namib desert fairy circles, *Science*, *339*(6127), 1618–1621.
Katra, I., H. Lavee, and S. Pariente (2008), The effect of rock fragment size and position on topsoil moisture on arid and semi-arid hillslopes, *Catena*, *72*, 49–55.
Katul, G., A. Porporato, and R. Oren (2007), Stochastic dynamics of plant-water interactions, *Annu. Rev. Ecol. Evol. Syst.*, *38*, 767–791.
Kéfi, S., M. B. Eppinga, P. C. de Ruiter, and M. Rietkerk (2010), Bistability and regular spatial patterns in arid ecosystems, *Theor. Ecol.*, *3*(4), 257–269.
Kéfi, S., M. Rietkerk, M. Roy, A. Franc, P. C. de Ruiter, and M. Pascual (2011), Robust scaling in ecosystems and the meltdown of patch size distributions before extinction, *Ecol. Lett.*, *14*(1), 29–35.
Kinast, S., Y. R. Zelnik, G. Bel, and E. Meron (2014), Interplay between turing mechanisms can increase pattern diversity, *Phys. Rev. Lett.*, *112*, 078701.
Meron, E. (2012), Pattern-formation approach to modelling spatially extended ecosystems, *Ecol. Modell.*, *234*(0), 70–82, doi:10.1016/j.ecolmodel.2011.05.035.
Midgley, G. F., and F. van der Heyden (1999), Form and function in perennial plants, in *The Karoo: Ecological Patterns and Processes*, chap. 6, pp. 91–106, edited by W. R. J. Dean and S. Milton, Cambridge Univ. Press, Cambridge, U. K.
Mulla, D. J., and A. B. McBratney (1999), Soil spatial variabity, in *Handbook of Soil Science*, chap. 9, 1st ed., pp. A321–A352, edited by M. E. Sumner, CRC Press, Boca Raton, Fla.
Noy-Meir, I. (1973), Desert ecosystems: Environment and producers, *Annu. Rev. Ecol. Syst.*, *4*, 25–51.
Pelletier, J. D., S. B. DeLong, C. A. Orem, P. Becerra, K. Compton, K. Gressett, J. Lyons-Baral, L. A. McGuire, J. L. Molaro, and J. C. Spinler (2012), How do vegetation bands form in dry lands? Insights from numerical modeling and field studies in southern Nevada, USA, *J. Geophys. Res.*, *117*, F04026, doi:10.1029/2012JF002465.
Picker, M. D., V. Ross-Gillespie, K. Vilieghe, and E. Moll (2012), Ants and the enigmatic Namibian fairy circles—Cause and effect?, *Ecol. Entomol.*, *37*, 33–42.
Puigdefabregas, J. (2005), The role of vegetation patterns in structuring runoff and sediment fluxes in drylands, *Earth Surf. Processes Landforms*, *30*, 133–147.
Puigdefabregas, J., A. Sol, L. Gutierrez, G. del Barrio, and M. Boer (1999), Scales and processes of water and sediment redistribution in drylands: Results from the Rambla Honda field site in SE Spain, *Earth Sci. Rev.*, *48*, 39–70.
Reynolds, J. F., et al. (2007), Global desertification: Building a science for dryland development, *Science*, *316*, 847–851.
Rietkerk, M. (1998), Catastrophic vegetation dynamics and soil degradation in semi-arid grazing systems, *in Tropical Re-source Management Papers*, *20*, Wageningen Agric. Univ., Wageningen, Netherlands.
Rietkerk, M., F. van den Bosch, and J. van de Koppel (1997), Site-specific properties and irreversible vegetation changes in semi-arid grazing systems, *Oikos*, *80*, 241–252.
Rietkerk, M., M. C. Boerlijst, F. van Langevelde, R. HilleRisLambers, J. van de Koppel, L. Kumar, H. H. T. Prins, and A. M. de Roos (2002), Self-organization of vegetation in arid ecosystems, *Am. Nat.*, *160*(4), 524–530.
Rietkerk, M., S. C. Dekker, P. C. de Ruiter, and J. van de Koppel (2004), Self-organized patchiness and catastrophic shifts in ecosystems, *Science*, *305*(5692), 1926–1929.
Rodríguez-Iturbe, I., and A. Porporato (2004), *Ecohydrology of Water-Controlled Ecosystems: Soil Moisture and Plant Dynamics*, Cambridge Univ. Press, Cambridge, U. K.
Saco, P. M., and M. Moreno-de las Heras (2013), Ecogeomorphic coevolution of semiarid hillslopes: Emergence of banded and striped vegetation patterns through interaction of biotic and abiotic processes, *Water Resour. Res.*, *49*, 115–126, doi:10.1029/2012WR012001.

Scheffer, M., J. Bascompte, W. A. Brock, V. Brovkin, S. R. Carpenter, V. Dakos, H. Held, E. H. van Nes, M. Rietkerk, and G. Sugihar (2009), Early-warning signals for critical transitions, *Nature*, *461*(7260), 53–59.

Schenk, H. J., and R. B. Jackson (2002), Rooting depths, lateral root spreads and below? ground/above-ground allometries of plants in water-limited ecosystems, *J. Ecol.*, *90*, 480–494.

Schlesinger, W. H., J. A. Raikes, A. E. Hartley, and A. F. Cross (1996), On the spatial pattern of soil nutrients in desert ecosystems, *Ecology*, *77*(2), 364–374.

Schwinning, S., and O. E. Sala (2004), Hierarchy of responses to resource pulses in arid and semi-arid ecosystems, *Oecologia*, *141*(2), 211–220.

Segoli, M., E. D. Ungar, and M. Shachak (2008), Shrubs enhance resilience of a semi-arid ecosystem by engineering and regrowth, *Ecohydrology*, *1*(4), 330–339.

Sela, S., T. Svoray, and S. Assouline (2012), Soil water content variability at the hillslope scale: Impact of surface sealing, *Water Resour. Res.*, *48*, W03522, doi:10.1029/2011WR011297.

Sheffer, E., J. von Hardenberg, H. Yizhaq, M. Shachak, and E. Meron (2013), Emerged or imposed: A theory on the role of physical templates and self-organisation for vegetation patchiness, *Ecol. Lett.*, *16*(2), 127–139.

Svoray, T., and A. Karnieli (2011), Rainfall, topography and primary production relationships in a semiarid ecosystem, *Ecohydrology*, *4*, 55–66.

Svoray, T., R. Shafran-Nathan, Z. Henkin, and A. Perevolotsky (2008), Spatially and temporally explicit modeling of conditions for primary production of annuals in dry environments, *Ecol. Modell.*, *218*, 339–353.

van Nes, E. H., and M. Scheffer (2005), Implications of spatial heterogeneity for catastrophic regime shifts in ecosystems, *Ecology*, *86*(7), 1797–1807.

van Wijngaarden, W. (1985), Elephants-trees-grass-grazers: Relationships between climate, soil, vegetation and large herbivores in a semi-arid savanna ecosystem, *ITC Pub. 4*, 165 pp., Int. Inst. for Aerospace Surv. and Earth Sci., Enschede, Netherlands.

Walker, B. H., D. Ludwig, C. S. Holling, and R. M. Peterman (1981), Stability of semi-arid savanna grazing systems, *J. Ecol.*, *69*, 473–498.

Zelnik, Y. R., S. Kinast, H. Yizhaq, G. Bel, and E. Meron (2013), Regime shifts in models of dryland vegetation, *Philos. Trans. R. Soc. A*, *371*, 20120358.